Persistent inward currents in tibialis anterior motoneurons can be reliably estimated within the same session

Journal of Electromyography and Kinesiology 78 (2024) 102911

Contents lists available at ScienceDirect

Journal of Electromyography and Kinesiology

journal homepage: www.elsevier.com/locate/jelekin

Persistent inward currents in tibialis anterior motoneurons can be reliably estimated within the same session

Thomas Lapole [a,*,1], Ricardo N.O. Mesquita [b,c,d,**,1], Stéphane Baudry [e], Robin Souron [f], Eleanor K. O'Brien [c,g], Callum G. Brownstein [h,2], Vianney Rozand [a,i,2]

[a] Laboratoire Interuniversitaire de Biologie de la Motricité, Université Jean Monnet Saint-Etienne, Lyon 1, Université Savoie Mont-Blanc, Saint-Etienne, France
[b] Department of Electrical Engineering, Chalmers University of Technology, Gothenburg, Sweden
[c] School of Medical and Health Sciences, Edith Cowan University, Perth, Australia
[d] Neuroscience Research Australia, Sydney, Australia
[e] Laboratory of Applied Biology, Research Unit in Applied Neurophysiology (LABNeuro), Faculty of Motor Sciences, Université Libre de Bruxelles (ULB), Belgium
[f] Nantes Université, Mouvement – Interactions – Performance, MIP, UR 4334, F-44000 Nantes, France
[g] Centre for Precision Health, Edith Cowan University, Perth, Western Australia, Australia
[h] Newcastle University, School of Biomedical, Nutritional and Sports Sciences, Newcastle-upon-Tyne, United Kingdom
[i] INSERM UMR1093-CAPS, Université Bourgogne Franche-Comté, UFR des Sciences du Sport, F-21000 Dijon, France

ARTICLE INFO

Keywords:
Neuromodulation
Serotonin
Noradrenaline
Motor neurone
Motor neuron

ABSTRACT

The response of spinal motoneurons to synaptic input greatly depends on the activation of persistent inward currents (PICs), the contribution of which can be estimated through the paired motor unit technique. Yet, the intra-session test–retest reliability of this measurement remains to be fully established. Twenty males performed isometric triangular dorsiflexion contractions to 20 and 50 % of maximal torque at baseline and after a 15-min resting period. High-density electromyographic signals (HD-EMG) of the tibialis anterior were recorded with a 64-electrode matrix. HD-EMG signals were decomposed, and motor units tracked across time points to estimate the contribution of PICs to motoneuron firing through quantification of motor unit recruitment-derecruitment hysteresis (ΔF). A good intraclass correlation coefficient (ICC = 0.75 [0.63, 0.83]) and a large repeated measures correlation coefficient (r_{rm} = 0.65 [0.49, 0.77]; $p < 0.001$) were found between ΔF values obtained at both time points for 20 % MVC ramps. For 50 % MVC ramps, a good ICC (0.77 [0.65, 0.85]) and a very large repeated measures correlation coefficient (r_{rm} = 0.73 [0.63, 0.80]; $p < 0.001$) were observed. Our data suggest that ΔF scores can be reliably investigated in tibialis anterior motor units during both low- and moderate-intensity contractions within a single experimental session.

1. Introduction

Human movement relies on the generation of force by skeletal muscles, a process intricately governed by the interplay between neural and muscular factors. The modulation of muscle force is achieved through modulation of the recruitment of motor units (MUs) and/or increases in their firing frequency. MU firing patterns depend on the synaptic integration occurring at the cell bodies of motoneurons. While voluntary commands from the motor cortex serve as the primary mean of activating alpha-motoneurons, multiple excitatory and inhibitory afferent inputs projecting onto motoneurons influence their activity. Moreover, motoneurons receive serotonergic (Bowker et al., 1981) and noradrenergic (Proudfit and Clark, 1991) inputs from the brainstem. The binding of these neuromodulators to metabotropic receptors initiates intracellular signalling cascades that modulate the properties of voltage-gated channels (i.e., intrinsic motoneuronal electrical properties) (Powers and Binder, 2001). The most evident neuromodulatory mechanism is the activation of persistent inward currents (PICs) (Heckman

* Corresponding author at: Laboratoire Interuniversitaire de Biologie de la Motricité, Université Jean Monnet Saint-Etienne, Lyon 1, Université Savoie Mont-Blanc, Saint-Etienne, France.
** Corresponding author at: Department of Electrical Engineering, Chalmers University of Technology, Maskingränd 2, Gothenburg, Sweden.
E-mail addresses: thomas.lapole@univ-st-etienne.fr (T. Lapole), mesquita@chalmers.se (R.N.O. Mesquita).
[1] Equal first authors.
[2] Equal senior authors.

https://doi.org/10.1016/j.jelekin.2024.102911
Received 27 February 2024; Received in revised form 9 May 2024; Accepted 6 June 2024
Available online 9 June 2024

et al., 2005, 2009). PICs amplify and prolong the effects of the ionotropic system, introducing non-linearities to the relationship between the net synaptic input to a motoneuron pool and the resulting motor output (Binder et al., 2020).

The contribution of PICs to motoneuron firing cannot be directly measured in humans. Nonetheless, distinct MU firing patterns have been observed which are likely generated by PICs (Heckman et al., 2005, 2009). During a slow linear increase of voluntary drive, initial firing acceleration and saturation are typically observed, followed by recruitment-derecruitment hysteresis (i.e., derecruitment occurs at a lower input level than recruitment) during a subsequent phase of slow decrease in voluntary output. These non-linear firing patterns have been identified *in vivo* during ramp contractions using decomposition of intramuscular electromyographic signals (e.g., Foley and Kalmar, 2019, Marchand-Pauvert et al., 2019, Revill and Fuglevand, 2017) and, more recently, high-density surface electromyographic signals (HD-EMG) (e.g., Hassan et al., 2021, Khurram et al., 2021, Orssatto et al., 2021). The paired MU technique (Gorassini et al., 2002, Gorassini et al., 1998) allows the estimation of the contribution of PICs to the prolongation of human motoneuron firing (i.e., recruitment-derecruitment hysteresis) during submaximal voluntary ramp contractions. During a ramp contraction, the smoothed firing frequency of a lower-threshold control MU is used as a proxy of net synaptic input. Thus, the strength of net synaptic input can then be estimated at the time of recruitment and derecruitment of a higher-threshold MU (test unit). The difference in the smoothed firing rate of the control unit at recruitment and derecruitment of the test unit constitutes the ΔF score (i.e., change in frequency). This method has been validated by intracellular direct PIC measurements in animal models (Bennett et al., 2001) and by computer simulations (Powers and Heckman, 2015). Yet, the test–retest reliability of such measurements has been only scarcely investigated with average scores per participant (Orssatto et al., 2023, Trajano et al., 2020). Using data from all extracted MUs while accounting for the nested structure of the data pertaining to PIC estimates is however imperative to provide a more accurate test of ΔF test–retest variability. Analytical approaches that consider the hierarchical nature of MU data without reducing data to averaged scores within individuals have already been used to assess effects of experimental interventions (e.g., Boccia et al., 2019, Mesquita et al., 2023).

The aim of the present study was to investigate the intra-session reliability of the estimated contribution of PICs to recruitment-derecruitment firing hysteresis (ΔF) using a linear mixed modelling approach that considers the nestedness typical of these types of data. As secondary objectives, we also investigated reliability of MU recruitment thresholds, derecruitment thresholds and firing rate, and examined whether ΔF scores varied across recruitment thresholds.

2. Methods

2.1. Participants

Data presented in this study were obtained from a previously published study where we investigated the ongoing and acute effects of local vibration on PICs estimated contribution to motoneuron firing (Lapole et al., 2023). Twenty male participants volunteered to participate in this study (age: 30 ± 7 yrs, height: 177.9 ± 7.0 cm, body mass: 76.5 ± 12.2 kg). Participants were asked to avoid caffeine and alcohol consumption as well as to abstain from strenuous exercise 24 h prior to the testing session. Participants provided written informed consent and this study conformed to the ethical standards set by the Declaration of Helsinki, except for registration in a database. The study was approved by the local research ethics committee (CPP SudEst I; 1408208-2015-A00036-43).

2.2. Design

Data collection was performed in a single session, with participants seating on a dynamometer and high-density electromyography (HD–EMG) measurements performed on the tibialis anterior (TA) of the right leg. After a familiarisation period to the experimental procedures, participants performed at least two 3-s maximal isometric voluntary dorsiflexion contractions (MVCs) with a 60-s inter-trial passive rest. Additional MVCs were performed until the difference between the two best trials was less than 5 %. Participants then performed triangular isometric contractions at baseline (CON-1) and were retested after a 15-min resting period (CON-2) to investigate the reliability of estimates of PIC contribution to motoneuron firing. In each time point, three triangular contractions were performed to both 20 and 50 % MVC, with the ascending and descending phase lasting 10 s each (i.e., 2 % of MVC.s^{-1} and 5 % of MVC.s^{-1}, respectively). Triangular contractions to the same intensity were interspaced by a 30-s rest, and contraction intensities were randomly ordered and separated by 1 min of passive rest.

2.3. Torque and electromyographic recordings

Dorsiflexion torque was measured during voluntary contractions using a calibrated instrumented pedal (CS1060 300 Nm; FGP Sensors, Les Clayes Sous Bois, France; Fig. 1). Participants were seated upright in a custom-built chair with hips at 90° of flexion (0° = neutral position), right knee at 120° of extension (180° = full extension) and right ankle in a neutral position. The foot was securely attached to the pedal with a custom-made hook and loop fastener. Participants were provided with real-time feedback of the torque trace displayed on a large screen. The peak isometric dorsiflexion torque was taken as the highest value during the MVCs and used to set the intensity of the ramp contractions.

The skin under the electrodes was shaved, abraded with sandpaper, and swabbed with alcohol. One flexible 64-electrode HD-EMG grid was placed on the TA muscle (13 rows x 5 columns). Electrodes had a 1-mm diameter and 8-mm inter-electrode distance (GR08MM1305; OT Bioelettronica, Turin, Italy). The location of the TA was identified through palpation before the array was placed on the muscle belly, with the grid covering most of the TA proximal area (Del Vecchio et al., 2019). The array was attached to the skin by bi-adhesive foam and the skin-to-electrode contact optimised by filling the wells of the adhesive foam with conductive cream (AC Cream, Spes Medica, Genoa, Italy). Strap

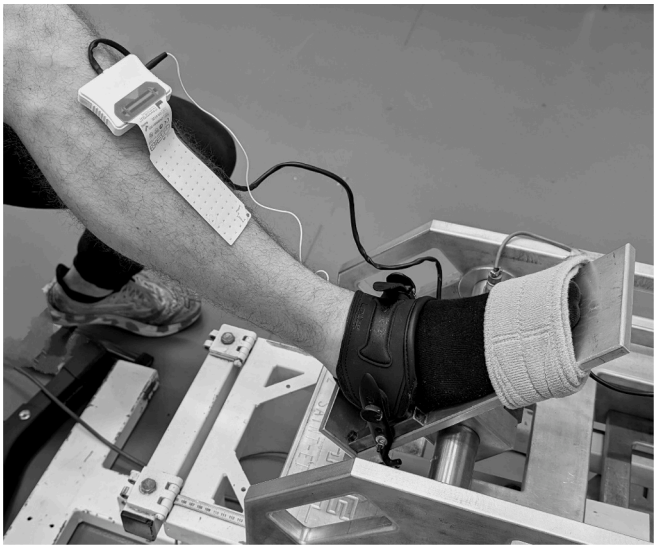

Fig. 1. Illustration of the instrumented pedal for dorsiflexion torque measurement and the 64-electrode HD-EMG grid placed on the tibialis anterior muscle.

electrodes dampened with water were placed around the ankle (ground electrode) and wrist (reference electrode). HD-EMG signals were amplified (150x), collected in monopolar mode, through a 16-bit A/D (Quattrocento; OT Bioelettronica, Torino, Italy), band-pass filtered (10–500 Hz) and digitised at a rate of 5120 Hz. EMG signals were recorded and visualised using OTBioLab+ software (version 1.4.2.0, OT Bioelettronica, Torino, Italy) throughout the protocol to ensure acceptable signal quality.

2.4. Data analysis

2.4.1. Motor unit identification and tracking

HD-EMG signals and torque recordings were converted from the OTBioLab+ format into MATLAB-compatible data files (Version R2021B, MathWorks, Natick, USA). These files were then processed offline with the DEMUSE software tool (v5.01; The University of Maribor, Slovenia) that relies on the convolutive blind source separation method (Holobar and Zazula, 2007). Band-pass zero-phase (20–500 Hz), zero-phase 2nd order finite impulse response high-pass differential (230 Hz), and notch (50 Hz and their higher harmonics) filters were applied in DEMUSE. For each subject, the three channels with the lowest signal-to-noise ratio were automatically removed to optimise decomposition, and 50 sequential decomposition runs were conducted in each ramp contraction independently. For each time point and contraction intensity (20 and 50 %), only the best ramp contraction was retained for analysis. Ramps were selected by the experimenter based on smoothness and adherence to the torque template, as well as the number of identified MUs (i.e. the more the better).

For each contraction intensity, the selected ramps were concatenated and the same MUs were tentatively tracked over the different time points. MU duplicates were removed and spike trains visually inspected and manually edited by a trained investigator (Del Vecchio et al., 2020). After editing, only MUs that presented a global pulse-to-noise ratio greater than 30 dB were retained for further analysis (Holobar et al., 2014).

2.4.2. Extraction of motor unit firing characteristics

After carefully editing the spike trains, firing events were converted into instantaneous firing rates and smoothed using a 5th order polynomial function, with additional MATLAB scripts and functions. All polynomials were visually inspected and if edge effects were observed at MU recruitment or derecruitment (i.e., a clear mismatch between the change in the smoothed and instantaneous firing rate), the MU from that specific trial was not included in further analyses. MU maximal firing rate was considered as the maximal value obtained from the polynomial curve (i.e., smoothed peak firing rate). Recruitment and derecruitment thresholds were also computed as the torque level (% MVC) at the time when the MU started and stopped firing action potentials, respectively.

We then used the paired MU technique (Gorassini et al., 2002, Gorassini et al., 1998) to estimate the contribution of PICs to TA motoneuron firing (see Lapole et al. (2023), Fig. 1). This technique quantifies MU recruitment-derecruitment hysteresis (i.e., ΔF). Lower-threshold MUs (i.e., control units) were paired with higher-threshold MUs (i.e., test units), with the smoothed firing frequency of control units being used as an estimate of changes in the net synaptic input. In each MU pair, the hysteresis of the test unit was quantified by calculating the difference between the smoothed firing rates of the control unit at recruitment and derecruitment of the test unit, which constitutes the ΔF (change in frequency) score (Gorassini et al., 2002). Criteria were used to test the assumption that the control unit was a suitable proxy for net synaptic input. Pairs were included if rate-to-rate Pearson's correlation coefficients between the smoothed firing rate polynomials of the test and control units (calculated from 5120 data points per second on Excel, Version 2019, Microsoft Corporation, USA) were $r > 0.7$ (Stephenson and Maluf, 2011), so as to ensure that control and test MUs likely shared a common synaptic drive. The first 500 ms of the test unit were excluded from the correlation analysis to minimise contamination of a non-linear firing rate acceleration at the time of recruitment (Mottram et al., 2009). Moreover, only pairs with a recruitment time difference greater than 1 s were considered to meet the assumption that PICs in the control unit were fully activated when the test unit was recruited, avoiding the contamination of the aforementioned non-linear firing rate acceleration (Hassan et al., 2020). Moreover, a MU pair was not considered for analysis if the test unit was derecruited before the control unit. Finally, a saturation criterion was used, excluding pairs in which the control unit did not increase its firing rate more than 0.5 Hz after the recruitment of the test unit, as the control unit would not be sensitive to changes in synaptic drive (Stephenson and Maluf, 2011).

The quantification of the variables that were needed for the ΔF calculation, as well as the identification of suitable pairs and calculation of ΔF values were conducted in Excel (Version 2019, Microsoft Corporation, Redmond, USA). Data were compared between CON-1 and CON-2 to investigate the reliability of ΔF measurements. Only pairs identified at the two time points were used for ΔF calculation. Importantly, ΔF scores were calculated for individual test units as the average value obtained when the units were paired with multiple suitable control units, as previously conducted (Trajano et al., 2020).

2.5. Statistical analysis

Analyses of MU variables were conducted in R (version 4.0.5), using RStudio environment (version 1.4.1106). Reliability analyses from the entire set of MUs were conducted by computing intraclass correlation coefficients (ICCs) and repeated measures correlations coefficients for ΔF scores, recruitment thresholds, derecruitment thresholds, and peak smoothed firing rates. To calculate ICCs, a linear mixed-effect model with random intercepts was computed (*lmerTest* package; Bates et al. (2015)). The model included a fixed intercept term and 'motor unit' nested within 'participant' were specified as random factors (*Variable* ~ *1 + (1|Participant/Motor_unit)*. ICCs were calculated by dividing the variance of interest by the total variance of the model (Nakagawa et al., 2017). Confidence intervals (95 %) for ICCs were calculated by bootstrapping. Values between 0 and 0.50 were considered as poor, 0.50 and 0.75 as moderate, 0.75 and 0.90 as good, and > 0.90 as excellent (Koo and Li, 2016). Repeated-measures correlations coefficients (r_{rm}) were also computed between CON-1 and CON-2 values using the *rmcorr* package (Bakdash and Marusich, 2017). Correlation magnitude was interpreted based on Cohen's criteria (Cohen, 2013): trivial, $r_{rm} < 0.1$; weak, $r_{rm} = 0.1$–0.3; moderate, $r_{rm} = 0.3$–0.5; large, $r_{rm} = 0.5$–0.7; very large, $r_{rm} = 0.7$–0.9; and nearly perfect, $r_{rm} > 0.9$. Furthermore, average scores per participant were also computed to calculate coefficients of variation (CVs) as the ratio between the standard deviation and the mean of individual measurements. This process was repeated for each participant, resulting in individual CV values for each MU variable during both 20 % and 50 % ramp contractions. To obtain an aggregated measure of the CV across participants, the mean of these individual CVs was then calculated for each parameter (Knutson et al., 1994).

Separate linear mixed-effects models were also used to examine whether ΔF scores, MU recruitment thresholds, MU derecruitment thresholds, and peak smoothed firing rates were significantly different between CON-1 and CON-2 (Boccia et al., 2019). Variables were analysed with a random intercept (parallel slopes) model using 'time point' as a fixed effect, and "motor unit' nested in 'participant' as random effects (*Variable ~ time_point + (1 | Participant/Motor_Unit)*. Residuals were plotted against fitted values to assess whether variance was consistent across the fitted range and Q-Q plot inspection was used to assess the assumption of normality of residuals. Estimated marginal means (with 95 % confidence intervals [CI]) were quantified (*emmeans* package; Lenth and Lenth (2018)). Significance was set at $p < 0.05$. Moreover, model-based estimates were used to calculate Cohen's d effect size for comparisons between both time points. Specifically, estimated marginal means from the linear mixed model (*emmeans* package)

were employed. The standardised mean difference was calculated as the difference between time point means divided by the residual standard deviation (sigma) from the fitted model. This approach uses the model's residual variance to account for the variability in the data and provides an effect size that reflects the underlying model structure. The magnitude of effect sizes was interpreted based on Cohen's criteria (Cohen, 2013): trivial for values between 0 and 0.2, small for 0.2–0.5, medium for 0.5–08, and large for > 0.8.

Finally, repeated measures correlations were also computed (*rmcorr* package; Bakdash and Marusich (2017)) to investigate an association between the magnitude of ΔF and MU recruitment threshold during both time points.

3. Results

3.1. Motor unit identification

MUs could not be identified in two out of 20 participants in all trials. Additionally, MUs could not be identified during 20 % MVC ramps in two additional participants, and during 50 % MVC ramps in two others. Therefore, data presented below are from 16 participants for both 20 and 50 % MVC ramps. A total of 260 (16.2 ± 9.4 per participant) and 256 (15.8 ± 8.6 per participant) MUs were tracked during 20 and 50 % MVC ramps, respectively, across both CON-1 and CON-2. Of those MUs, a total of 27 (1.7 ± 2.0 per participant) and 20 (1.3 ± 1.5 per participant) MUs exhibited edge effects and were excluded from analysis.

3.2. Reliability of ΔF measurements

A total of 84 test units (5.6 ± 3.6 per participant) and 468 pairs (31.2 ± 44.9 per participant; representing 23 % of the total number of potential pairs) were successfully tracked during both ramp contractions (CON-1 and CON-2) performed at 20 % MVC. In one participant, we were unable to track any pair between CON-1 and CON-2 (n = 15). During 50 % MVC ramps, we successfully tracked 141 test units (8.4 ± 5.9 per participant) and 794 pairs (55.8 ± 68.9 per participant; representing 39 % of the total number of potential pairs) during both contractions (CON-1 and CON-2).

There was no significant change of ΔF from CON-1 to CON-2 for both 20 % ($F_{(1,83)} = 3.0$; $p = 0.08$; $d = 0.27$) and 50 % MVC ramps ($F_{(1,140)} = 0.07$; $p = 0.80$; $d = 0.031$) (Table 1). In 20 % ramps, a mean difference of + 0.2 Hz [-0.03, 0.4] was observed. The mean difference in 50 % ramps was + 0.03 Hz [-0.2, 0.3]. Moreover, ICCs of ΔF values were good for both 20 % and 50 % ramps (Table 2). There was also a large repeated measures correlation for 20 % MVC ramps (Fig. 2A), and a very large repeated measures correlation for 50 % MVC ramps (Fig. 2B).

3.3. Reliability of motor units' thresholds and firing rate

When considering recruitment threshold values obtained for all the identified MUs, values were significantly decreased from CON-1 to CON-2 for 20 % ($F_{(1,233)} = 16.8$; $p < 0.001$; $d = 0.38$) and were significantly increased from CON-1 to CON-2 for 50 % MVC ramp contractions ($F_{(1,233)} = 20.0$; $p < 0.001$; $d = 0.41$) (Table 1). Estimated mean differences from CON-1 to CON-2 were −0.6 % MVC [-0.3, −0.9] and + 1.1 % MVC [0.6, 1.6], respectively. Yet, ICC was good for 20 % MVC ramps and excellent for 50 % MVC ramps (Table 2). Moreover, we observed a nearly perfect repeated-measures correlation between recruitment threshold values obtained in CON-1 and CON-2 for both 20 % and 50 % MVC ramps (Table 2).

Similar results were observed for derecruitment threshold (Table 1). Values were significantly increased between the two time points for both 20 % ($F_{(1,233)} = 4.7$; $p = 0.03$; $d = 0.20$) and 50 % MVC ramp contractions ($F_{(1,233)} = 27.2$; $p < 0.001$; $d = 0.48$). Estimated mean differences from CON-1 to CON-2 were + 0.3 % MVC [0.03, 0.5] and + 1.2 % MVC [0.7, 1.6], respectively. ICCs were however good and excellent for 20 and 50 % MVC ramps, respectively (Table 2). Moreover, nearly perfect repeated-measures correlation coefficients were observed between values obtained in CON-1 and CON-2 for both 20 % and 50 % MVC ramps (Table 2).

For smoothed peak firing rate (Table 1), values were significantly decreased between the two time points for 50 % MVC contractions ($F_{(1,233)} = 15.7$; $p < 0.001$; $d = 0.37$) with an estimated mean difference from CON-1 to CON-2 of −0.4 Hz [-0.2, −0.7]. No difference was observed for 20 % MVC contractions ($F_{(1,233)} = 0.3$; −0.04 Hz [-0.2, 0.09]; $p = 0.56$; $d = 0.054$). ICCs were excellent and good for 20 and 50 % MVC ramps, respectively (Table 2). There was a nearly perfect correlation between values obtained in CON-1 and CON-2 for 20 % MVC ramps while it was very large for 50 % MVC ramps (Table 2).

3.4. Correlations between recruitment threshold of test units and ΔF values

In 20 % MVC ramps, ΔF was moderately associated with the recruitment threshold of test units in both CON-1 ($r_{rm} = 0.42$ [0.21, 0.60]; $p < 0.001$) and CON-2 ($r_{rm} = 0.47$ [0.26, 0.64]; $p < 0.001$) (Fig. 3). In 50 % MVC ramps, a small correlation was observed in CON-2 ($r_{rm} = 0.22$ [0.05, 0.38]; $p = 0.01$) but not in CON-1 ($r_{rm} = 0.05$ [-0.13, 0.22]; $p = 0.61$) (Fig. 3).

4. Discussion

Our results showed good ICC values and large to very large repeated-measures correlations between ΔF values obtained at two time points separated by 15 min of rest. Similarly, good to excellent ICC values and very large to nearly perfect correlations were observed for MU firing rate and both recruitment and derecruitment thresholds, despite a significant difference between the two time points. These results indicate that ΔF can be reliably investigated in TA motoneurons during both low- and moderate-intensity contractions. These findings hold particular importance given that (1) ΔF scores from a single contraction are often used in comparisons between control and experimental conditions (e.g., Goodlich et al., 2023a, Orssatto et al., 2022), and (2) decomposition of HD-EMG signals from the tibialis anterior are commonly used to compute ΔF scores (e.g., Beauchamp et al., 2023, Goodlich et al., 2023a, Goreau et al., 2024, Jenz et al., 2023, Orssatto et al., 2022, Trajano et al., 2023).

Table 1
Motor units' characteristics recorded during ramp contractions performed to 20 % and 50 % of maximal voluntary force (MVC) in both control time points (i.e., CON-1 and CON-2). Data are presented as estimated marginal mean with 95 % confidence intervals [CI].

		CON-1		CON-2		p value
20 %	**ΔF score (Hz)**	4.6	[4.0, 5.1]	4.8	[4.2, 5.3]	0.08
	Recruitment threshold (% MVC)	6.8	[5.6, 8.1]	6.2	[5.0, 7.4]	**<0.001**
	Derecruitment threshold (% MVC)	6.8	[6.0, 7.5]	7.0	[6.3, 7.8]	**0.03**
	Smoothed peak firing rate (Hz)	15.1	[14.1, 16.1]	15.0	[14.1, 16.0]	0.56
50 %	**ΔF score (Hz)**	5.4	[4.7, 6.1]	5.4	[4.7, 6.1]	0.80
	Recruitment threshold (% MVC)	23.6	[19.6, 27.5]	24.6	[20.7, 28.6]	**<0.001**
	Derecruitment threshold (% MVC)	24.4	[20.7, 28.2]	25.6	[21.9, 29.3]	**<0.001**
	Smoothed peak firing rate (Hz)	20.2	[18.9, 21.6]	19.8	[18.4, 21.1]	**<0.001**

Table 2
Reliability of motor units' characteristics recorded during ramp contractions performed to 20 % and 50 % of maximal voluntary force. 95 % confidence intervals [CI] for intraclass correlation coefficients (ICC) and repeated measures correlation coefficients (r_{rm}) are indicated between brackets. Coefficient of variation (CV) values are indicated as mean and standard deviation across participants.

		ICC		r_{rm}		CV
20 %	**ΔF score**	0.75	[0.63, 0.83]	0.65	[0.49, 0.77]	13.4 ± 10.0 %
	Recruitment threshold	0.86	[0.82, 0.89]	0.93	[0.91, 0.95]	31.3 ± 15.1 %
	Derecruitment threshold	0.84	[0.80, 0.87]	0.92	[0.90, 0.94]	19.8 ± 8.1 %
	Smoothed peak firing rate	0.92	[0.85, 0.94]	0.92	[0.89, 0.94]	3.6 ± 2.0 %
50 %	**ΔF score**	0.77	[0.65, 0.85]	0.73	[0.63, 0.80]	15.9 ± 8.4 %
	Recruitment threshold	0.95	[0.94, 0.96]	0.98	[0.97, 0.98]	16.6 ± 15.6 %
	Derecruitment threshold	0.96	[0.94, 0.97]	0.98	[0.97, 0.98]	12.0 ± 10.5 %
	Smoothed peak firing rate	0.83	[0.73, 0.89]	0.88	[0.84, 0.91]	5.0 ± 4.3 %

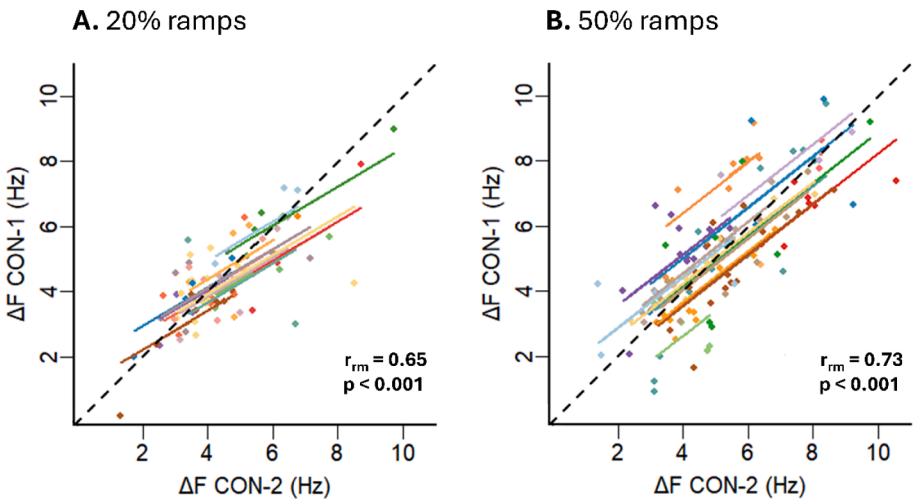

Fig. 2. Repeated-measures correlation (r_{rm}) plots illustrating the association between ΔF scores in both CON-1 and CON-2. Left panel (A) shows data from ramp contractions performed to 20 % of maximal voluntary contraction (MVC) torque and right panel (B) shows data from ramp contractions performed to 50 % MVC. Each colour represents a single participant and parallel lines are fitted to test units from each participant. A line of identity is depicted in a dashed black line, representing where the values on the x-axis and y-axis would be equal. ΔF scores present a large correlation between time points in the 20 % MVC ramps, and a very large correlation in the 50 % MVC ramps.

Few studies previously investigated intra-session (Goodlich et al., 2023b, Hoshizaki et al., 2020, Martinez-Valdes et al., 2016, Trajano et al., 2020) and inter-session (e.g., Colquhoun et al., 2018, Goodlich et al., 2023b, Hoshizaki et al., 2020, Martinez-Valdes et al., 2017) reliability of MU variables computed from HD-EMG decomposition. To the best of our knowledge, only two studies have examined intra-session (Trajano et al., 2020) and inter-session (Orssatto et al., 2023) reliability outcomes (i.e., ICC) of ΔF measurements. In an effort to address limitations of the statistical approaches employed in previous MU studies, our reliability analyses utilised the entire set of computed scores (i.e., rather than an average score per participant), thereby enhancing statistical power while taking into consideration the nested structure of the data (i.e., multiple MUs per participant) (Galbraith et al., 2010, Moen et al., 2016). This is particularly crucial given that MU firing values are highly correlated within a participant, even across testing days (Tenan et al., 2014), and given the significant variability in the number of extracted MUs among participants (Oliveira et al., 2022). To this end, ICCs, calculated as the between-observation variance as a proportion of the total variance from a mixed model approach were calculated (Nakagawa et al., 2017), and repeated-measures correlations (Bakdash and Marusich, 2017) used for the examination of reliability levels. Moreover, CV values, a widely accepted reliability index within the scientific community, were reported. However, a note of caution is due here, as average scores per participant were used to compute CVs, adhering to a reduced data approach to maintain the assumption of independence between observations.

As ΔF computation depends on MU firing characteristics, intra-session reliability of other variables was also calculated. Recruitment and derecruitment thresholds and smoothed firing rate obtained in CON-1 and CON-2 presented good to excellent ICC values, and repeated-measures correlations were very large to nearly perfect for both low (i.e., 20 % MVC) and moderate (i.e., 50 % MVC) triangular ramp contractions. To the best of our knowledge, this is the first study to report reliability indices (i.e. ICC, repeated-measures correlation coefficients, and CV values) of threshold values recorded on a large number of MUs through HD-EMG. Moreover, the reliability levels for smoothed peak firing rate in this study align consistently with previous research, which has demonstrated good to excellent intra-session reliability (Hoshizaki et al., 2020, Martinez-Valdes et al., 2016, Trajano et al., 2020). Despite good reliability, our results showed small differences in threshold and firing rates values across the two measured time points, except for smoothed peak firing rate during 20 % MVC ramps. Fluctuations in threshold values across trials of the same contraction type have already been reported by Romaiguere et al. (1993) using intramuscular EMG. This led the authors to suggest that MUs have a range of force over which they can be recruited or derecruited rather than a set force value. The observed differences in MU characteristics between contractions of similar characteristics can be partly due to the multiple combinations of muscle activation patterns that can be used to accomplish the same task (i.e., muscle redundancy (Latash et al., 2010)), leading to variability in the recruitment and firing patterns of MUs. Accordingly, the firing behaviour of a given MU will depend on the number of previously recruited MUs and their firing frequencies. Any changes in MU behaviour might provoke adjustments in voluntary drive to ensure that the

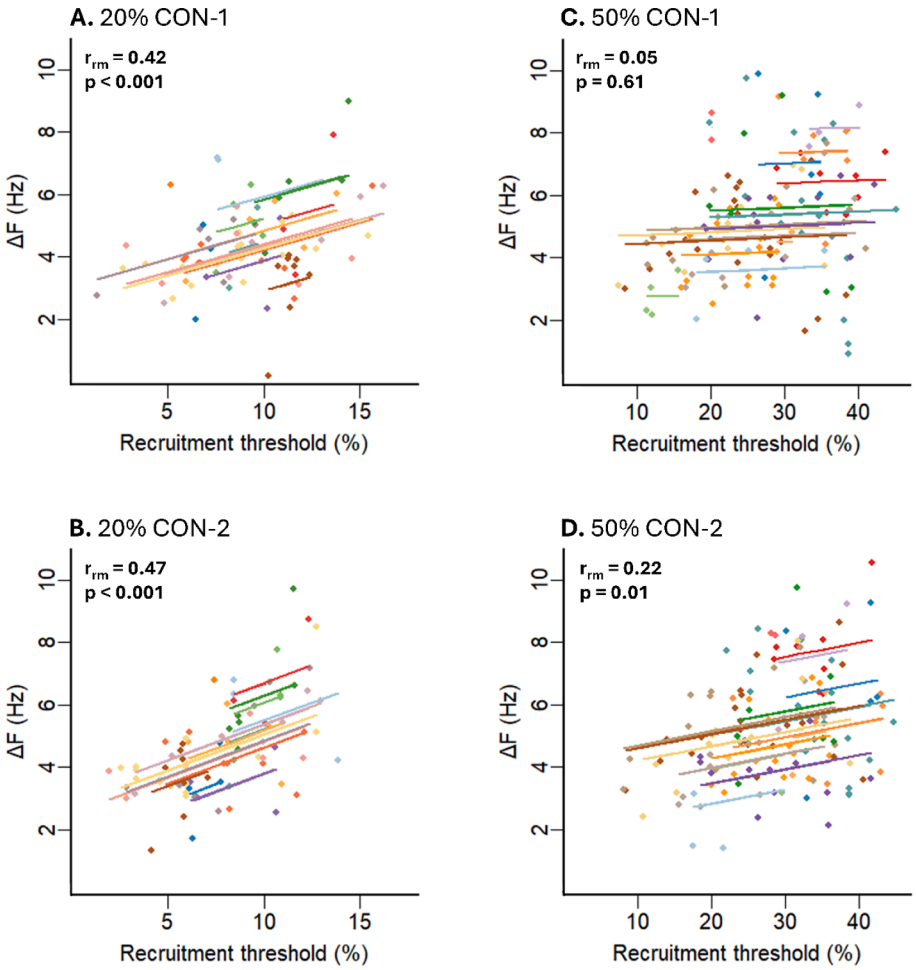

Fig. 3. Repeated-measures correlation (r_{rm}) plots illustrating the association between recruitment threshold of test units and ΔF values. CON-1 is presented in panels A and B. CON-2 is presented in panels B and D. Values during ramp contractions performed to 20 % of maximal voluntary contraction (MVC) are presented in panels A and B. Values during ramp contractions to 50 % MVC are presented in panels C and D. Each colour represents a single participant and parallel lines are fitted to test units from each participant. Except for 50 % MVC ramps in CON-1, weak to moderate positive correlations were observed, suggesting greater ΔF scores in test units with higher recruitment-thresholds.

task is performed accurately. Moreover, MUs identified through decomposition of HD-EMG represent a relatively small portion of the total number of motoneurons actively contributing to the contraction (Farina et al., 2010), with a bias towards MUs with the largest surface action potentials (see range of recruitment thresholds in Fig. 3). MU firing behaviour is also dependent on the contribution of synergistic and antagonist muscles. The impact of these unidentified MUs on the firing pattern of the identified MUs and the resulting force remains unknown and prevent a clear interpretation of the observed changes in MU parameters. Lastly, although differences in thresholds and peak smoothed firing rates were statistically significant, their functional significance may be limited. The observed differences were relatively marginal, as indicated by the trivial and small effect sizes, and as further supported by comparing those differences to the range of values that can be observed during a wide range of contraction intensities (Connelly et al., 1999).

Interestingly, while there were some significant differences in MUs' thresholds as well as smoothed peak firing rate, such differences were not observed for ΔF, which exhibited relatively low estimated mean differences between control time points (+0.2 Hz and + 0.03 Hz for 20 % and 50 % MVC ramps, respectively). Accordingly, our reliability examinations revealed good ICC values, a large repeated-measures correlation between CON-1 and CON-2 ΔF values during 20 % MVC ramps, and very large during 50 % MVC ramps. Although different statistical approaches were used, these results for the TA muscle are consistent with the high ICC values previously reported for the soleus and gastrocnemius medialis muscles in an intra-session design (Trajano et al., 2020), as well as for the TA in an inter-session examination (Orssatto et al., 2023). Collectively, these outcomes suggest that estimates of PICs can be reliably investigated through the paired MU technique during both low- and moderate-intensity contractions. This holds significance as ΔF as small as 0.58 Hz have recently been associated with large increases in peak firing rates and with moderate to very large improvements in motor function (Orssatto et al., 2023). It is important to acknowledge, however, that our focus was only on the intra-session reliability of ΔF scores. Future studies should then investigate its inter-session reliability while taking advantage of the large samples of MU data provided by HD-EMG decomposition and concurrently considering the nested structure of these large datasets. Moreover, only male participants were enrolled in the present study and our reliability results cannot therefore be directly generalised to females.

Finally, we provide evidence that ΔF scores may depend on the recruitment threshold of the MU. Correlations between ΔF scores and the recruitment threshold of test units was only evident (i.e., moderate correlation) in 20 % MVC ramps (Fig. 3A and 3B), with this correlation being either small or absent for 50 % MVC ramps (Fig. 3C and 3D). Our findings partly suggest that there is a tendency for greater magnitudes of suprathreshold PICs in motoneurons of larger sizes. This possibility is consistent with animal studies (Huh et al., 2017, Lee and Heckman, 1998, Sharples and Miles, 2021), one human study in which MUs were

identified from intramuscular recordings (Stephenson and Maluf, 2011), and another human study in which multiple MUs were identified from HD-EMG signals (Beauchamp et al., 2023). However, it is contrary to three studies of multiple human MUs identified from HD-EMG signals (Afsharipour et al., 2020, Mesquita et al., 2023, Mesquita et al., 2022) and some animal evidence (Li et al., 2004). Future studies should continue to explore whether contribution of PICs to motoneuron firing varies with human motoneuron size and respective implications in motor output.

5. Conclusion

The present study showed that the estimated contribution of PICs to motoneuron firing (ΔF) can be reliably investigated within the same experimental session in TA motoneurons during both low- and moderate-intensity contractions in male participants. Moreover, our data suggest that motoneurons recruited at low levels of force may exhibit less recruitment-derecruitment hysteresis in triangular contractions, in comparison with motoneurons recruited at higher levels of force.

Authors contribution

T.L., RNO.M, CG.B and V.R. conceived and designed the research; T. L., CG.B and V.R. performed experiments; T.L., RNO.M, CG.B, V.R. and EK O. analysed data; T.L., RNO.M, S.B. R.S., CG.B and V.R. interpreted the results of experiments; T.L. and RNO.M. prepared figures; T.L. and RNO.M drafted the manuscript; all authors edited and revised the manuscript. All authors approved the final version of the manuscript and agreed to be accountable for all aspects of the work in ensuring that questions related to the accuracy or integrity of any part of the work are appropriately investigated and resolved. All persons designated as authors qualify for authorship, and all those who qualify for authorship are listed.

CRediT authorship contribution statement

Thomas Lapole: Writing – review & editing, Writing – original draft, Methodology, Investigation, Formal analysis, Data curation, Conceptualization. **Ricardo N.O. Mesquita:** Writing – review & editing, Writing – original draft, Formal analysis, Conceptualization. **Stéphane Baudry:** Writing – review & editing, Validation. **Robin Souron:** Writing – review & editing, Validation. **Eleanor K. O'Brien:** Writing – review & editing, Validation, Software. **Callum G. Brownstein:** Writing – review & editing, Methodology, Formal analysis, Data curation, Conceptualization. **Vianney Rozand:** Writing – review & editing, Validation, Methodology, Data curation, Conceptualization.

Declaration of competing interest

The authors declare that they have no known competing financial interests or personal relationships that could have appeared to influence the work reported in this paper.

Acknowledgments

We thank Franck Le Mat for his assistance on statistical analysis. This work was funded by the Jean Monnet University of Saint-Etienne through funding of the high-density electromyography device, allowing a 6-month teaching discharge to T.L. to work on this study.

References

Afsharipour, B., Manzur, N., Duchcherer, J., Fenrich, K.F., Thompson, C.K., Negro, F., Quinlan, K.A., Bennett, D.J., Gorassini, M.A., 2020. Estimation of self-sustained activity produced by persistent inward currents using firing rate profiles of multiple motor units in humans. J. Neurophysiol. 124 (1), 63–85.

Bakdash, J.Z., Marusich, L.R., 2017. Repeated measures correlation. Front. Psychol. 8, 456.

Bates, D., Mächler, M., Bolker, B., Walker, S., 2015. Fitting Linear Mixed-Effects Models Usinglme4. J. Stat. Softw. 67 (1).

Beauchamp, J.A., Pearcey, G.E.P., Khurram, O.U., Chardon, M., Wang, Y.C., Powers, R. K., Dewald, J.P.A., Heckman, C.J., 2023. A geometric approach to quantifying the neuromodulatory effects of persistent inward currents on individual motor unit discharge patterns. J. Neural Eng. 20 (1).

Bennett, D.J., Li, Y., Harvey, P.J., Gorassini, M., 2001. Evidence for plateau potentials in tail motoneurons of awake chronic spinal rats with spasticity. J. Neurophysiol. 86 (4), 1972–1982.

Binder, M.D., Powers, R.K., Heckman, C.J., 2020. Nonlinear Input-Output Functions of Motoneurons. Physiology 35 (1), 31–39.

Boccia, G., Martinez-Valdes, E., Negro, F., Rainoldi, A., Falla, D., 2019. Motor unit discharge rate and the estimated synaptic input to the vasti muscles is higher in open compared with closed kinetic chain exercise. J. Appl. Physiol. 127 (4), 950–958.

Bowker, R.M., Westlund, K.N., Coulter, J.D., 1981. Serotonergic projections to the spinal cord from the midbrain in the rat: an immunocytochemical and retrograde transport study. Neurosci. Lett. 24 (3), 221–226.

Cohen, J., 2013. Statistical Power Analysis for the Behavioral Sciences, second ed.

Colquhoun, R.J., Tomko, P.M., Magrini, M.A., Muddle, T.W.D., Jenkins, N.D.M., 2018. The influence of input excitation on the inter- and intra-day reliability of the motor unit firing rate versus recruitment threshold relationship. J. Neurophysiol. 120 (6), 3131–3139.

Connelly, D.M., Rice, C.L., Roos, M.R., Vandervoort, A.A., 1999. Motor unit firing rates and contractile properties in tibialis anterior of young and old men. J. Appl. Physiol. 87 (2), 843–852.

Del Vecchio, A., Negro, F., Holobar, A., Casolo, A., Folland, J.P., Felici, F., Farina, D., 2019. You are as fast as your motor neurons: speed of recruitment and maximal discharge of motor neurons determine the maximal rate of force development in humans. J. Physiol. 597 (9), 2445–2456.

Del Vecchio, A., Holobar, A., Falla, D., Felici, F., Enoka, R.M., Farina, D., 2020. Tutorial: Analysis of motor unit discharge characteristics from high-density surface EMG signals. J. Electromyogr. Kinesiol. 53, 102426.

Farina, D., Holobar, A., Merletti, R., Enoka, R.M., 2010. Decoding the neural drive to muscles from the surface electromyogram. Clin. Neurophysiol. 121 (9), 1616–1623.

Foley, R.C.A., Kalmar, J.M., 2019. Estimates of persistent inward current in human motor neurons during postural sway. J. Neurophysiol. 122 (5), 2095–2110.

Galbraith, S., Daniel, J.A., Vissel, B., 2010. A study of clustered data and approaches to its analysis. J. Neurosci. 30 (32), 10601–10608.

Goodlich, B.I., Del Vecchio, A., Horan, S.A., Kavanagh, J.J., 2023a. Blockade of 5-HT2 receptors suppresses motor unit firing and estimates of persistent inward currents during voluntary muscle contraction in humans. J. Physiol. 601 (6), 1121–1138.

Goodlich, B.I., Del Vecchio, A., Kavanagh, J.J., 2023b. Motor unit tracking using blind source separation filters and waveform cross-correlations: reliability under physiological and pharmacological conditions. J. Appl. Physiol. 135 (2), 362–374.

Gorassini, M.A., Bennett, D.J., Yang, J.F., 1998. Self-sustained firing of human motor units. Neurosci. Lett. 247 (1), 13–16.

Gorassini, M., Yang, J.F., Siu, M., Bennett, D.J., 2002. Intrinsic activation of human motoneurons: possible contribution to motor unit excitation. J. Neurophysiol. 87 (4), 1850–1858.

Goreau, V., Hug, F., Jannou, A., Dernoncourt, F., Crouzier, M., Cattagni, T., 2024. Estimates of persistent inward currents in lower limb muscles are not different between inactive, resistance-trained, and endurance-trained young males. J. Neurophysiol. 131 (2), 166–175.

Hassan, A.S., Fajardo, M.E., Cummings, M., McPherson, L.M., Negro, F., Dewald, J.P.A., Heckman, C.J., Pearcey, G.E.P., 2021. Estimates of persistent inward currents are reduced in upper limb motor units of older adults. J. Physiol. 599 (21), 4865–4882.

Hassan, A., Thompson, C.K., Negro, F., Cummings, M., Powers, R.K., Heckman, C.J., Dewald, J.P.A., McPherson, L.M., 2020. Impact of parameter selection on estimates of motoneuron excitability using paired motor unit analysis. J. Neural Eng. 17 (1), 016063.

Heckman, C.J., Gorassini, M.A., Bennett, D.J., 2005. Persistent inward currents in motoneuron dendrites: implications for motor output. Muscle Nerve 31 (2), 135–156.

Heckman, C.J., Mottram, C., Quinlan, K., Theiss, R., Schuster, J., 2009. Motoneuron excitability: the importance of neuromodulatory inputs. Clin. Neurophysiol. 120 (12), 2040–2054.

Holobar, A., Minetto, M.A., Farina, D., 2014. Accurate identification of motor unit discharge patterns from high-density surface EMG and validation with a novel signal-based performance metric. J. Neural Eng. 11 (1), 016008.

Holobar, A., Zazula, D., 2007. Multichannel Blind Source Separation Using Convolution Kernel Compensation. IEEE Trans. Signal Process. 55 (9), 4487–4496.

Hoshizaki, T., Clancy, E.A., Gabriel, D.A., Green, L.A., 2020. The reliability of surface EMG derived motor unit variables. J. Electromyogr. Kinesiol. 52, 102419.

Huh, S., Siripuram, R., Lee, R.H., Turkin, V.V., O'Neill, D., Hamm, T.M., Heckman, C.J., Manuel, M., 2017. PICs in motoneurons do not scale with the size of the animal: a possible mechanism for faster speed of muscle contraction in smaller species. J. Neurophysiol. 118 (1), 93–102.

Jenz, S.T., Beauchamp, J.A., Gomes, M.M., Negro, F., Heckman, C.J., Pearcey, G.E.P., 2023. Estimates of persistent inward currents in lower limb motoneurons are larger in females than in males. J. Neurophysiol. 129 (6), 1322–1333.

Khurram, O.U., Negro, F., Heckman, C.J., Thompson, C.K., 2021. Estimates of persistent inward currents in tibialis anterior motor units during standing ramped contraction tasks in humans. J. Neurophysiol. 126 (1), 264–274.

Knutson, L.M., Soderberg, G.L., Ballantyne, B.T., Clarke, W.R., 1994. A study of various normalization procedures for within day electromyographic data. J. Electromyogr. Kinesiol. 4 (1), 47–59.
Koo, T.K., Li, M.Y., 2016. A Guideline of Selecting and Reporting Intraclass Correlation Coefficients for Reliability Research. J. Chiropr. Med. 15 (2), 155–163.
Lapole, T., Mesquita, R.N.O., Baudry, S., Souron, R., Brownstein, C.G., Rozand, V., 2023. Can local vibration alter the contribution of persistent inward currents to human motoneuron firing? J. Physiol. 601 (8), 1467–1482.
Latash, M.L., Levin, M.F., Scholz, J.P., Schoner, G., 2010. Motor control theories and their applications. Medicina (Kaunas) 46 (6), 382–392.
Lee, R.H., Heckman, C.J., 1998. Bistability in spinal motoneurons in vivo: systematic variations in rhythmic firing patterns. J. Neurophysiol. 80 (2), 572–582.
Lenth, R., Lenth, M.R., 2018. Package 'lsmeans'. Am. Stat. 34 (4), 216–221.
Li, Y., Gorassini, M.A., Bennett, D.J., 2004. Role of persistent sodium and calcium currents in motoneuron firing and spasticity in chronic spinal rats. J. Neurophysiol. 91 (2), 767–783.
Marchand-Pauvert, V., Peyre, I., Lackmy-Vallee, A., Querin, G., Bede, P., Lacomblez, L., Debs, R., Pradat, P.F., 2019. Absence of hyperexcitability of spinal motoneurons in patients with amyotrophic lateral sclerosis. J. Physiol. 597 (22), 5445–5467.
Martinez-Valdes, E., Laine, C.M., Falla, D., Mayer, F., Farina, D., 2016. High-density surface electromyography provides reliable estimates of motor unit behavior. Clin. Neurophysiol. 127 (6), 2534–2541.
Martinez-Valdes, E., Negro, F., Laine, C.M., Falla, D., Mayer, F., Farina, D., 2017. Tracking motor units longitudinally across experimental sessions with high-density surface electromyography. J. Physiol. 595 (5), 1479–1496.
Mesquita, R.N.O., Taylor, J.L., Trajano, G.S., Skarabot, J., Holobar, A., Goncalves, B.A. M., Blazevich, A.J., 2022. Effects of reciprocal inhibition and whole-body relaxation on persistent inward currents estimated by two different methods. J. Physiol. 600 (11), 2765–2787.
Mesquita, R.N.O., Taylor, J.L., Trajano, G.S., Holobar, A., Goncalves, B.A.M., Blazevich, A.J., 2023. Effects of jaw clenching and mental stress on persistent inward currents estimated by two different methods. Eur. J. Neurosci. 58 (9), 4011–4033.
Moen, E.L., Fricano-Kugler, C.J., Luikart, B.W., O'Malley, A.J., 2016. Analyzing Clustered Data: Why and How to Account for Multiple Observations Nested within a Study Participant? PLoS One 11 (1), e0146721.
Mottram, C.J., Suresh, N.L., Heckman, C.J., Gorassini, M.A., Rymer, W.Z., 2009. Origins of abnormal excitability in biceps brachii motoneurons of spastic-paretic stroke survivors. J. Neurophysiol. 102 (4), 2026–2038.
Nakagawa, S., Johnson, P.C.D., Schielzeth, H., 2017. The coefficient of determination R (2) and intra-class correlation coefficient from generalized linear mixed-effects models revisited and expanded. J. Roy. Soc., Interface / Roy. Soc. 14 (134).
Oliveira, D.S., Casolo, A., Balshaw, T.G., Maeo, S., Lanza, M.B., Martin, N.R.W., Maffulli, N., Kinfe, T.M., Eskofier, B.M., Folland, J.P., Farina, D., Del Vecchio, A., 2022. Neural decoding from surface high-density EMG signals: influence of anatomy and synchronization on the number of identified motor units. J. Neural Eng. 19 (4).
Orssatto, L.B.R., Mackay, K., Shield, A.J., Sakugawa, R.L., Blazevich, A.J., Trajano, G.S., 2021. Estimates of persistent inward currents increase with the level of voluntary drive in low-threshold motor units of plantar flexor muscles. J. Neurophysiol. 125 (5), 1746–1754.
Orssatto, L.B.R., Fernandes, G.L., Blazevich, A.J., Trajano, G.S., 2022. Facilitation-inhibition control of motor neuronal persistent inward currents in young and older adults. J. Physiol. 600 (23), 5101–5117.
Orssatto, L.B.R., Rodrigues, P., Mackay, K., Blazevich, A.J., Borg, D.N., Souza, T.R., Sakugawa, R.L., Shield, A.J., Trajano, G.S., 2023. Intrinsic motor neuron excitability is increased after resistance training in older adults. J. Neurophysiol. 129 (3), 635–650.
Powers, R.K., Binder, M.D., 2001. Input-output functions of mammalian motoneurons. Rev. Physiol. Biochem. Pharmacol. 143, 137–263.
Powers, R.K., Heckman, C.J., 2015. Contribution of intrinsic motoneuron properties to discharge hysteresis and its estimation based on paired motor unit recordings: a simulation study. J. Neurophysiol. 114 (1), 184–198.
Proudfit, H.K., Clark, F.M., 1991. The projections of locus coeruleus neurons to the spinal cord. Prog. Brain Res. 88, 123–141.
Revill, A.L., Fuglevand, A.J., 2017. Inhibition linearizes firing rate responses in human motor units: implications for the role of persistent inward currents. J. Physiol. 595 (1), 179–191.
Romaiguere, P., Vedel, J.P., Pagni, S., 1993. Comparison of fluctuations of motor unit recruitment and de-recruitment thresholds in man. Exp. Brain Res. 95 (3), 517–522.
Sharples, S.A., Miles, G.B., 2021. Maturation of persistent and hyperpolarization-activated inward currents shapes the differential activation of motoneuron subtypes during postnatal development. Elife 10.
Stephenson, J.L., Maluf, K.S., 2011. Dependence of the paired motor unit analysis on motor unit discharge characteristics in the human tibialis anterior muscle. J. Neurosci. Methods 198 (1), 84–92.
Tenan, M.S., Marti, C.N., Griffin, L., 2014. Motor unit discharge rate is correlated within individuals: a case for multilevel model statistical analysis. J. Electromyogr. Kinesiol. 24 (6), 917–922.
Trajano, G.S., Taylor, J.L., Orssatto, L.B.R., McNulty, C.R., Blazevich, A.J., 2020. Passive muscle stretching reduces estimates of persistent inward current strength in soleus motor units. J. Exp. Biol. 223 (Pt 21).
Trajano, G.S., Orssatto, L.B.R., McCombe, P.A., Rivlin, W., Tang, L., Henderson, R.D., 2023. Longitudinal changes in intrinsic motoneuron excitability in amyotrophic lateral sclerosis are dependent on disease progression. J. Physiol. 601 (21), 4723–4735.